Acoustic waves and the detectability of first-order phase transitions by eLISA

IOP Conf. Series: Journal of Physics: Conf. Series **840** (2017) 012031 doi:10.1088/1742-6596/840/1/012031

Acoustic waves and the detectability of first-order phase transitions by eLISA

David J. Weir

Department of Physics and Helsinki Institute of Physics,
FI-00014 University of Helsinki, Finland

E-mail: david.weir@helsinki.fi

Abstract. In various extensions of the Standard Model it is possible that the electroweak phase transition was first order. This would have been a violent process, involving the formation of bubbles and associated shock waves. Not only would the collision of these bubbles and shock waves be a detectable source of gravitational waves, but persistent acoustic waves could enhance the signal and improve prospects of detection by eLISA. I summarise the results of a recent campaign to model such a phase transition based on large-scale hydrodynamical simulations, and its implications for the eLISA mission.

1. Introduction

The direct observation of gravitational waves from an astrophysical source [1] has also increased interest in direct observation of cosmological, stochastic sources of gravitational radiation. These include inflation and the processes which take place at the end of inflation, dynamics of networks of cosmic strings, and – perhaps most promisingly for future space-based gravitational wave detectors – first-order thermal phase transitions. Such a phase transition at the electroweak scale is perhaps the most promising cosmological source of directly observable gravitational waves.

A first-order phase transition proceeds by the nucleation and collision of bubbles of the new phase [2]. These bubbles may experience friction due to the bubble dynamics taking place in a bath of lighter particles. These interactions can slow the bubble walls considerably, so that they move subsonically in the medium of the plasma. Interactions between the plasma and the bubble can also, in principle at least, facilitate baryogenesis (see Ref. [3] for a recent review).

In the Standard Model, the electroweak phase transition has long been known to be a crossover [4, 5, 6], but it is quite easy to find extended models in which a first-order phase transition is possible. This therefore motivates thorough study of the processes and observable consequences of a first-order phase transition. One such consequence is the production of gravitational waves.

In the following sections I will summarise the various sources considered in the eLISA Cosmology Working Group report [7], as well as the ongoing efforts to simulate and model the underlying processes.

We assume that the phase transition took quickly on the scale of the expansion history of the universe. In the sections that follow, we will consider the energy density in gravitational waves $h^2\Omega_{\rm GW}$. This depends on a number of parameters, which we summarise here. We assume

that the gravitational waves are produced when the universe is at a temperature T_*, and that this can be assumed to be the same as the nucleation temperature. The system initially has g_* relativistic degrees of freedom. The nucleation rate β is then usually quoted relative to the Hubble rate H_* when the universe has temperature T_*. The terminal wall velocity of the bubbles is v_w. Energy densities are usually expressed in terms of three ratios. First, the ratio of vacuum energy to radiation energy is $\alpha = \rho_\mathrm{vac}/\rho_\mathrm{rad}$. This quantity is typically combined with the efficiencies of conversion into fluid and scalar gradient energy, defined as $\kappa_v = \rho_v/\rho_\mathrm{vac}$ and $\kappa_\phi = \rho_\phi/\rho_\mathrm{vac}$ respectively. Analogously, one can also define the efficiency of conversion into turbulent flow, $\kappa_\mathrm{turb} \approx 0.05\kappa_v$.

With the above quantities, usually calculable from phenomenological studies of the phase transition in a given model [8], we can make predictions about the expected gravitational radiation that will result, and that is our focus here.

In this short summary, the dynamics of the thermal phase transition will be separated into three stages: the initial collision of the bubbles, the acoustic waves set up as the bubbles collide, and then the onset of turbulence. We take each of these phenomena in turn and come up with a fiducial form of the gravitational wave power spectrum informed by the latest simulation results, before turning our attention briefly to how these relate to predictions for specific models.

2. The envelope approximation and beyond

Most predictions of gravitational wave power spectra from first-order phase transitions make use of a set of approximations which, taken together, are termed the 'envelope approximation' [9, 10, 11]. This assumes that the shell of stress-energy around the bubbles (whether gradient energy of the bubble wall or fluid kinetic energy in the plasma) is very thin on the scale of the bubble radii, and that the collision happens instantaneously at any point on the bubble surface. It is also assumed that the stress energy disappears and does not propagate into the interior of the merged bubble – in other words, that the 'envelope' of the bubble is all that matters.

These assumptions seem to work well for bubbles where there is no plasma – for example, a near-vacuum phase transition – but they are not adequate to describe the full physics of the shock waves that develop around the bubbles. Therefore we take the envelope approximation to account only for the bubble walls colliding. Their contribution to the gravitational wave power spectrum is approximately

$$h^2\Omega_\phi(f) = 1.67\times10^{-5}\left(\frac{H_*}{\beta}\right)^2\left(\frac{\kappa_\phi\alpha}{1+\alpha}\right)^2\left(\frac{100}{g_*}\right)^{\frac{1}{3}}\frac{0.11v_\mathrm{w}^3}{0.42+v_\mathrm{w}^2}S_\mathrm{env}(f) \tag{1}$$

with $S_\mathrm{env}(f)$ determined from semi-numerical evaluations of the envelope approximation,

$$S_\mathrm{env}(f) = \frac{(p+q)(f/f_\mathrm{env})^q}{1+q(f/f_\mathrm{env})^{p+q}} \tag{2}$$

with a rising power law $q \approx 3$ and falling power law $p \approx 1$ (Ref. [7] takes $q = 2.8$ and $p = 1$). There is some detail in the peak structure which may make these indices slightly smaller. The frequency f_env is set by the size of the bubbles at the time of collision, which is itself a function of the nucleation rate β and wall velocity v_w.

Figure 1 shows that the envelope approximation works well for large numbers of colliding scalar field bubble walls, for $v_\mathrm{w} < 1$.

One could replace κ_ϕ with κ_v to get an estimate of the gravitational waves from colliding shocks; indeed, this was for a long time the standard approach. However, it was demonstrated explicitly in Ref. [12] that the qualitative shape of the envelope approximation gravitational wave power spectrum is incorrect, because the acoustic wave source rapidly dominates.

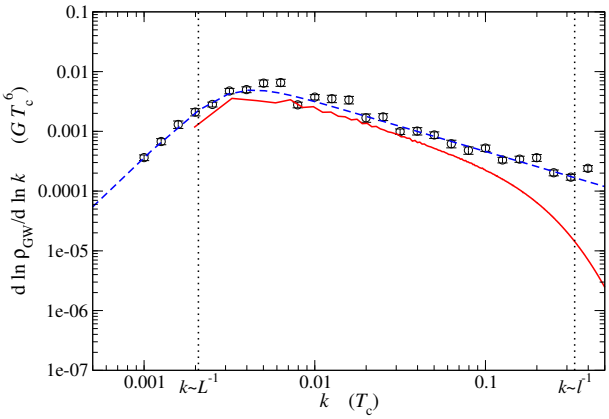

Figure 1. Plot comparing the gravitational wave energy density (which we denote $\rho_{\rm GW}$ here) from colliding scalar field walls ($v_{\rm w} = 0.44$) at the time of the phase transition as measured by two different simulation techniques. The envelope approximation result (square symbols, fit to dashed blue curve) is compared to a lattice simulation of a field-fluid system where the metric perturbations are sourced by the scalar field (solid red line). Where the two simulations are comparable, the envelope approximation adequately describes the collision of the scalar field bubble walls, although this is not usually the dominant source in a realistic scenario. For more information and the parameters used, see Ref. [12].

3. Acoustic waves

We cannot, therefore, treat the plasma shocks that surround each bubble by assuming that all the fluid kinetic energy lies in an infinitesimally thin region. Furthermore, we cannot assume that the kinetic energy dissipates immediately after the bubbles have collided. On the contrary, the collision is just the start [13, 14, 15]. After the bubbles have collided, the shock waves are no longer tied to the bubble wall and so slow down (or speed up) to move with the speed of sound in the medium.

These acoustic waves continue to interact and overlap, until expansion, shear viscosity or turbulence substantially change the dynamics. Generically it is the expansion of the universe that attenuates this source, on much longer timescales than the phase transition. The source appears stationary from the creation of the acoustic waves until this time. We concentrate on this stationary source of gravitational waves here, ignoring the initial transient effects.

We have carried out large-scale simulations of a model consisting of a relativistic scalar field, modelling the Higgs, coupled to a relativistic ideal fluid, modelling the plasma. Our most recent simulations of this system used up to simulation volumes up to 4200^3 points and took around a million core-hours per run [16].

Based on fits to our simulation results (see Fig. 2), we give the gravitational wave power as approximately

$$h^2\Omega_{\rm sw}(f) = 2.65 \times 10^{-6} \left(\frac{H_*}{\beta}\right) \left(\frac{\kappa_v \alpha}{1+\alpha}\right)^2 \left(\frac{100}{g_*}\right)^{\frac{1}{3}} v_{\rm w} S_{\rm sw}(f). \tag{3}$$

The form of $S_{\rm sw}(f)$ is the same as that for Eq. 2,

$$S_{\rm sw}(f) = \frac{(p+q)(f/f_{\rm sw})^q}{1+q(f/f_{\rm sw})^{p+q}} \tag{4}$$

but this time we take $q = 3$ and $p = 4$. The peak frequency $f_{\rm sw}$ here is likely to be quite close

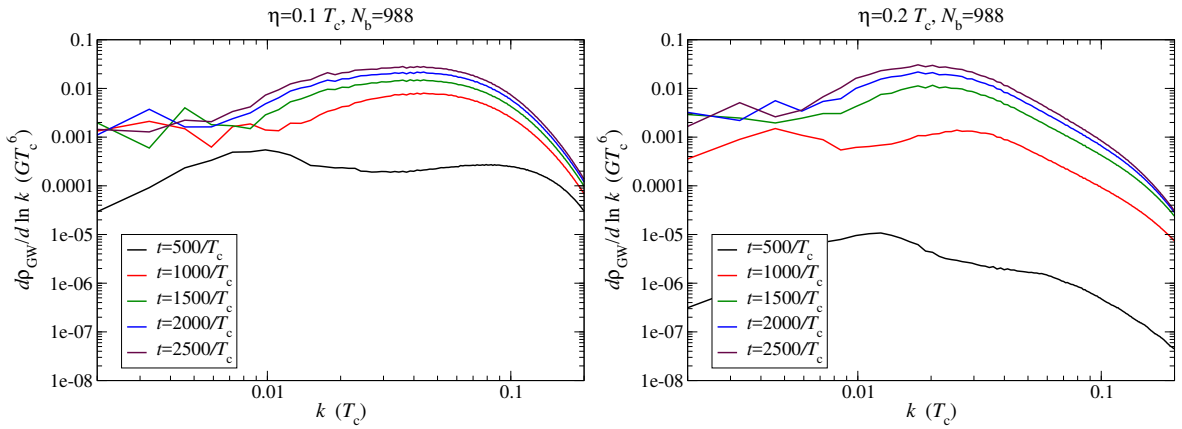

Figure 2. Gravitational wave power spectra for two example cases. At left is a simulation with wall velocity $v_w = 0.83$, a detonation; at right is a simulation with $v_w = 0.44$, a deflagration. Results like these were used to produce the fitting ansatz Eq. 3. For full details of the simulation parameters and interpretation of the results, see Ref. [14].

to f_{env}, but could differ by an order of magnitude, depending on the thickness of the fluid shell associated with the bubble wall.

The resulting gravitational wave power spectrum has a steeper high-frequency power law than the envelope approximation described above, although the overall amplitude is much higher, for a generic thermal phase transition. Work remains to be done on establishing the exact power law index but we expect to see $p \in [3, 4]$.

4. Turbulence

A thermal phase transition dumps energy into the plasma on long length scales. However, the kinetic and magnetic Reynolds numbers of the plasma are likely to be very large and so turbulence will develop in the plasma. This in turn amplifies magnetic fields and produces MHD turbulence [17]. Both turbulent processes redistribute the energy supplied to the plasma by the phase transition onto shorter length scales until a stationary spectrum is reached. The resulting gravitational wave power spectrum is [17, 18]

$$h^2\Omega_{\rm turb}(f) = 3.35\times10^{-4}\left(\frac{H_*}{\beta}\right)\left(\frac{\kappa_{\rm turb}\alpha}{1+\alpha}\right)^{\frac{3}{2}}\left(\frac{100}{g_*}\right)^{\frac{1}{3}} v_w S_{\rm turb}(f) \tag{5}$$

where the shape function $S_{\rm turb}(f)$ is rather different from the broken power law form for $S_{\rm sw}$ and $S_{\rm env}$, with a dependence on the Hubble rate h_* due to the duration of the source,

$$S_{\rm turb}(f) = \frac{(f/f_{\rm turb})^3}{[1+(f/f_{\rm turb})]^{\frac{11}{3}}(1+8\pi f/h_*)}. \tag{6}$$

The characteristic frequency $f_{\rm turb}$, like $f_{\rm sw}$ and $f_{\rm env}$, depends on the average bubble radius at the time of collision, amongst other considerations.

In addition to our use of an ideal fluid without viscosity, the length scales captured by and duration of our simulations are currently insufficient to capture the onset of turbulent behaviour (see Fig. 3), so we are reliant upon these analytical results and treat them as a totally separate source from the acoustic waves above.

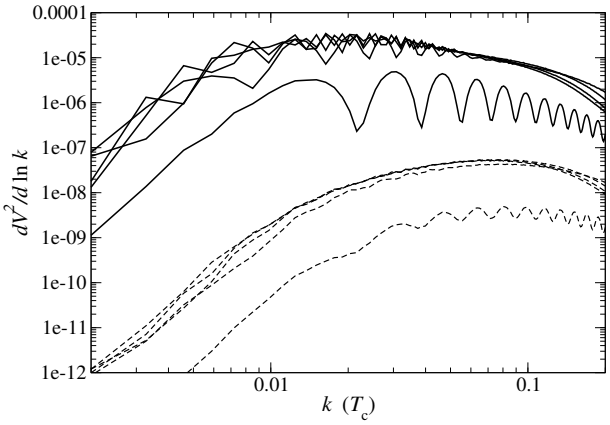

Figure 3. Comparison between rotational and longitudinal parts of the fluid velocity power spectrum computed in the simulations discussed in the main text. The viscosity, length scales and the duration of the simulation are insufficient to model the development of turbulence and so we rely on well-established analytic results from the literature [17]. The simulation parameters are the same as used to produce the plot in Fig. 2, right, and the curves are separated by the same time intervals.

5. Putting it all together

We combine the three sources described above, taking into account their relative magnitude for the scenario of interest,

$$h^2\Omega_{\rm GW}(f) = h^2\Omega_{\phi}(f) + h^2\Omega_{\rm sw}(f) + h^2\Omega_{\rm turb}(f). \tag{7}$$

As an example of this process, in Fig. 4 the gravitational wave power spectrum for an example of a strong, relativistic thermal phase transition is shown, along with the sensitivity curves for several eLISA mission profiles.

Note that this simple addition of the three sources neglects some subtleties. The initial collision of the fluid shock profiles is not modelled separately, and is assumed to be less important than either the colliding scalar field walls or the acoustic source. In addition, the onset of turbulence is ignored, which will in reality modulate the acoustic source. Finally, in simulations there is little separation between length scales and so considerable extrapolation is required to the large separation between wall thickness and bubble radius that would actually exist in a realistic electroweak phase transition.

6. Conclusions

We have summarised recent work on simulating and modelling the processes which take place in a thermal phase transition, as well as recent efforts to turn the results of those simulations into meaningful predictions for LISA.

The key result is that a wide variety of models and scenarios are detectable by LISA, perhaps wider than previously anticipated. The acoustic source being more significant than the mere collision of fluid shells (to which the envelope approximation was previously most commonly applied) would suggest. The result is an enhancement of order $60\beta/H_*$ in $h^2\Omega_{\rm GW}$.

Much remains to be done: the onset of turbulence has not been modelled; the power laws arising from acoustic waves need to be better understood; and the qualitative results are mostly from numerical simulations. Nevertheless there is cause for optimism in the ability of LISA to detect a very wide variety of first-order phase transitions at or around the electroweak scale. It should prove to be an important tool for high energy physics in the coming decades.

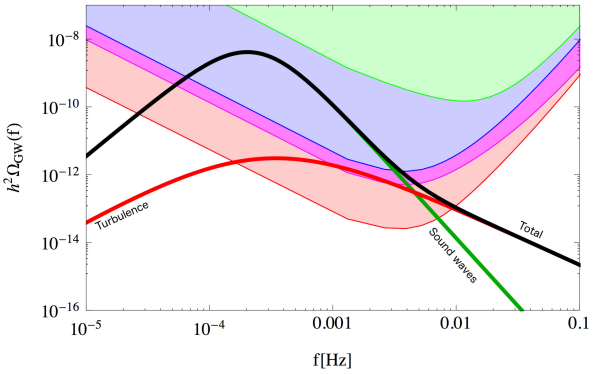

Figure 4. Gravitational wave power spectrum with transition temperature $T_* = 100\,\mathrm{GeV}$, $\alpha_{T_*} = 0.5$, $v_\mathrm{w} = 0.5$ and $\beta/H_* = 10$. For this parameter choice, the acoustic source is substantially responsible for the potential detectability of such a transition. Further details can be found in Ref. [7].

Acknowledgments

I am grateful to my collaborators Mark Hindmarsh, Stephan Huber and Kari Rummukainen for their collaboration on much of the simulation work summarised above. I am also grateful to my collaborators within the eLISA Cosmology Working Group and its coordinators, Chiara Caprini and Germano Nardini. I acknowledge PRACE for awarding access to resource HAZEL HEN based in Germany at the High Performance Computing Center Stuttgart (HLRS). My work was supported by the People Programme (Marie Skłodowska-Curie actions) of the European Union Seventh Framework Programme (FP7/2007-2013) under grant agreement number PIEF-GA-2013-629425. This research was supported by the Munich Institute for Astro- and Particle Physics (MIAPP) of the DFG cluster of excellence "Origin and Structure of the Universe".

References

[1] Abbott B P *et al.* 2016 *Phys. Rev. Lett.* **116** 061102 (*Preprint* 1602.03837)
[2] Steinhardt P J 1982 *Phys. Rev* D **25** 2074
[3] Morrissey D E and Ramsey-Musolf M J 2012 *New J. Phys.* **14** 125003 (*Preprint* 1206.2942)
[4] Kajantie K, Laine M, Rummukainen K and Shoposhnikov M E 1996 *Phys. Rev. Lett.* **77** 2887 (*Preprint* hep-ph/9605288)
[5] Gurtler M, Ilgenfritz E M and Schiller A 1997 *Phys. Rev.* D **56** 3888 (*Preprint* hep-lat/9704013)
[6] Csikor F, Fodor Z and Heitger J 1999 *Phys. Rev. Lett* **82** 21 (*Preprint* hep-ph/9809291)
[7] Caprini C *et al.* 2016 *J. Cosmol. Astropart. Phys.* JCAP04(2016)001 (*Preprint* 1512.06239)
[8] Espinosa J R, Konstandin T, No J M and Servant G 2010 *J. Cosmol. Astropart. Phys.* JCAP06(2010)028 (*Preprint* 1004.4187)
[9] Kosowsky A, Turner M S and Watkins R 1992 *Phys. Rev. Lett.* **69** 2026
[10] Kamionkowski M, Kosowsky A and Turner M S 1994 *Phys. Rev.* D **49** 2837 (*Preprint* astro-ph/9310044)
[11] Huber S J and Konstandin T 2008 *J. Cosmol. Astropart. Phys.* JCAP09(2008)022 (*Preprint* 0806.1828)
[12] Weir D J 2016 *Phys. Rev.* D **93** 124037 (*Preprint* 1604.08429)
[13] Hindmarsh M, Huber S J, Rummukainen K and Weir D J 2014 *Phys. Rev. Lett* **112** 041301 (*Preprint* 1304.2433)
[14] Hindmarsh M, Huber S J, Rummukainen K and Weir D J 2015 *Phys Rev.* D **92** 123009 (*Preprint* 1504.03291)
[15] Hindmarsh M 2016 *Preprint* 1608.04735
[16] Hindmarsh M, Huber S J, Rummukainen K and Weir D J (*In preparation*)
[17] Caprini C, Durrer R and Servant G 2009 *J. Cosmol. Astropart. Phys.* JCAP12(2009)024 (*Preprint* 0909.0622)
[18] Binetruy P, Bohe A, Caprini C and Dufaux J F 2012 *J. Cosmol. Astropart. Phys* JCAP06(2012)027 (*Preprint* 1201.0983)